Mol Neurobiol (2015) 51:610–622
DOI 10.1007/s12035-014-8740-7

Amyloid-Beta Disrupts Calcium and Redox Homeostasis in Brain Endothelial Cells

Ana Catarina R. G. Fonseca · Paula I. Moreira · Catarina R. Oliveira · Sandra M. Cardoso · Paolo Pinton · Cláudia F. Pereira

Received: 28 February 2014 / Accepted: 5 May 2014 / Published online: 16 May 2014

Abstract In Alzheimer's disease, the accumulation of amyloid-beta (Aβ) in the brain occurs in the parenchyma and cerebrovasculature. Several evidences support that the neuronal demise is potentiated by vascular alterations in the early stages of the disease, but the mechanisms responsible for the dysfunction of brain endothelial cells that underlie these cerebrovascular changes are unknown. Using rat brain microvascular endothelial cells, we found that short-term treatment with a toxic dose of $A\beta_{1\text{-}40}$ inhibits the Ca^{2+} refill and retention ability of the endoplasmic reticulum and enhances the mitochondrial and cytosolic response to adenosine triphosphate (ATP)-stimulated endoplasmic reticulum Ca^{2+} release. Upon prolonged $A\beta_{1\text{-}40}$ exposure, Ca^{2+} homeostasis was restored concomitantly with a decrease in the levels of proteins involved in its regulation operating at the plasma membrane, endoplasmic reticulum, and mitochondria. Along with perturbations in Ca^{2+} regulation, an early increase in the levels of oxidants and a decrease in the ratio between reduced and oxidized glutathione were observed in $A\beta_{1\text{-}40}$-treated endothelial cells. Under these conditions, the nuclear levels of oxidative stress-related transcription factors, namely, hypoxia-inducible factor 1α and nuclear factor (erythroid-derived 2)-related factor 2, were enhanced as well as the protein levels of target genes. In conclusion, $A\beta_{1\text{-}40}$ affects several mechanisms involved in Ca^{2+} homeostasis and impairs the redox homeostasis simultaneously with stimulation of protective stress responses in brain endothelial cells. However, the imbalance between cell death and survival pathways leads to endothelial dysfunction that in turn contributes to cerebrovascular impairment in Alzheimer's disease.

Keywords Brain microvascular endothelial cells · Endoplasmic reticulum · Mitochondria · Calcium homeostasis · Oxidative stress · Alzheimer's disease

Introduction

Several evidences show that accumulation of amyloid-beta (Aβ) occurs in the brain parenchyma and in the cerebrovasculature in Alzheimer's disease (AD) and suggest that neurovascular dysfunction plays a major role in the neurodegenerative process and cognitive decline [1–5]. Vascular pathology develops early and before the first symptoms in AD and correlates with changes in the blood-brain barrier [3]. Although the clearance of Aβ across the blood-brain barrier is considered to be deficient in the AD brain [6], other mechanisms such as cerebral Aβ degradation mediated by proteases such as neprilysin and insulin-degrading enzyme seem to play a major role and is supported by studies such as those by Iwatsubo and colleagues performed in AD patients and transgenic mice [7–10]. Deposition of Aβ in cerebral vasculature of AD transgenic mice and AD patients correlates with age-dependent dysfunction of brain capillary endothelium

A. C. R. G. Fonseca · P. I. Moreira · C. R. Oliveira · S. M. Cardoso · C. F. Pereira (✉)
Center for Neuroscience and Cell Biology, University of Coimbra, Largo Marquês de Pombal, 3004-517 Coimbra, Portugal
e-mail: cpereira@cnc.cj.uc.pt

A. C. R. G. Fonseca
Department of Life Sciences, Faculty of Science and Technology, University of Coimbra, Calçada Martim de Freitas, 3000-456 Coimbra, Portugal

P. I. Moreira · C. R. Oliveira · S. M. Cardoso · C. F. Pereira
Faculty of Medicine, University of Coimbra, Rua Larga, 3004-504 Coimbra, Portugal

P. Pinton
Department of Morphology, Surgery and Experimental Medicine; Section of Pathology, Oncology and Experimental Biology; Interdisciplinary Center for the Study of Inflammation (ICSI); Laboratory for Technologies of Advanced Therapies (LTTA), University of Ferrara, Ferrara, Italy

[11–13]. Although parenchymal diffuse and neuritic plaques have preferentially the $A\beta_{1-42}$ isoform, vascular deposits contain levels of $A\beta_{1-40}$ much higher than those of $A\beta_{1-42}$ [12]. In addition, the toxicity of Aβ on endothelial cells was well demonstrated in animals, isolated vessels, and cultured cells [14–17]. Aβ-induced vasoconstriction, which was demonstrated in ex situ human cerebral arteries and brain microvessels [18], seems to contribute to the reduced cerebral blood flow and consequent delay in oxygen and glucose transport to the brain during mild cognitive impairment and in AD [19]. The rat brain endothelial cells were shown to be more sensitive to oxygen and glucose deprivation than hippocampal neurons, and the subsequent activation of hypoxia-inducible factor 1α (HIF-1α) was found to increase Aβ production contributing to the described AD-related blood-brain barrier dysfunction [20].

The deregulation of Ca^{2+} homeostasis has been reported in different cell types from AD brain patients and also in animal and in vitro models of the disease [21–24]. Endoplasmic reticulum (ER) Ca^{2+} homeostasis is disturbed by some of the most frequent familial AD-associated mutations in presenilins, which function as passive Ca^{2+} leak channels in the ER membrane [25–27]. Recent studies demonstrate that familial mutations perturb the function of the mitochondrial-associated membranes and also suggest an important role for ER-mitochondria contacts and crosstalk in sporadic AD pathology [28, 29]. Moreover, lymphocytes from mild cognitive impairment and sporadic AD patients are more prone to inositol 1,4,5-trisphosphate (IP_3) receptor (IP_3R) activation, have an enhanced magnitude of Ca^{2+} influx during store-operated Ca^{2+} entry (SOCE) that is activated upon ER Ca^{2+} depletion, and, consequently, have increased cytosolic Ca^{2+} levels [30, 31]. In cultured cortical neurons, $A\beta_{1-40}$ was shown to significantly deplete ER Ca^{2+} leading to mitochondrial membrane depolarization, release of cytochrome c and activation of apoptosis-related caspases [32], and also to increase IP_3R and voltage-dependent anion channel (VDAC) protein expression as well as the number of ER-mitochondria contact points and mitochondrial Ca^{2+} concentrations [28]. Recently, we demonstrated that $A\beta_{1-40}$ induces ER stress in brain endothelial cells and triggers a mitochondria-mediated apoptotic cell death pathway involving ER-to-mitochondria Ca^{2+} transfer, decrease of mitochondrial membrane potential, and release of pro-apoptotic factors [33].

Deregulated Ca^{2+} homeostasis is associated with the production of reactive oxygen species (ROS) in numerous cell types under pathological conditions. For instance, mitochondrial depolarization due to mitochondrial Ca^{2+} overload disrupts the electron transport chain, increasing ROS generation [34]. Besides, mitochondrial Ca^{2+} can activate NADPH oxidase leading to the formation of free radicals and lipid peroxidation that deplete the antioxidant glutathione (GSH) [35]. Recent findings in yeast demonstrated that ROS production under mitochondrial dysfunction conditions is mediated by the ER resident NADPH oxidase [36]. Since capillary endothelial cells have a relatively high number of mitochondria, these cells are very susceptible to oxidative stress [37]. In addition to mitochondria, endothelial cells have other sources of ROS such as the endothelial nitric oxide synthase that produces nitric oxide in the presence of high Ca^{2+} levels [38]. On the other hand, ROS also deregulate Ca^{2+} homeostasis. For instance, ROS increase the response of IP_3Rs to cytosolic IP_3, activate or inhibit ryanodine receptors (RyRs) depending on ROS concentration, inhibit SOCE-associated Orai1, and alter the activity of voltage-gated Ca^{2+} channels and sarco/endoplasmic reticulum Ca^{2+}-ATPase (SERCA) [39].

Although low levels of ROS regulate cell survival signaling pathways, high levels of ROS cause cell damage and are involved in many neurodegenerative diseases, including AD [40–43]. Increased amounts of intracellular ROS have been found in different cell types exposed to Aβ and in AD animal models [42, 44], and, in turn, ROS promote the production of Aβ [45]. Increased ROS levels and endothelial cell-to-cell transmission are associated with apoptosis and disruption of the blood-brain barrier [46, 47]. Endothelial cells have several mechanisms to counteract the rise of ROS, including the translocation to the nucleus of transcription factors that regulate antioxidant genes, such as the nuclear factor (erythroid-derived 2)-related factor 2 (Nrf2, the master regulator of antioxidant genes) and hypoxia-inducible factor 1-alpha (HIF-1α, the master regulator of cellular adaptation to hypoxia), and the subcellular distribution of antioxidants such as GSH and superoxide dismutase [48]. However, ROS production can overwhelm the normal antioxidant capacity of the cells that can also be diminished by exogenous factors or by the accumulation of damaging agents as occurs during the aging process [48].

In order to better understand the mechanisms implicated in brain endothelial cells' dysfunction in AD, the perturbation of Ca^{2+} and redox homeostasis was investigated in cells from rat brain microvessels treated with levels of $A\beta_{1-40}$ previously demonstrated to be toxic. Data revealed time-dependent alterations in Ca^{2+} concentration in the cytosol, ER, and mitochondria upon $A\beta_{1-40}$ exposure that were correlated with oxidative stress markers and changes in proteins that are involved in the regulation of Ca^{2+} homeostasis at the ER-plasma membrane and ER-mitochondria level and activation of oxidative stress responses. These results provide new insights into the deleterious effects of $A\beta_{1-40}$ in brain endothelial cells that can be useful to the development of new therapies to prevent or delay the onset of AD.

Experimental Procedures

Materials

Mem-Alpha medium with Glutamax-1, Nut Mix F-10 W/GLUTAMAX-1, fetal bovine serum (FBS), geneticin, and enhanced chemiluminescent (ECL) were acquired from Invitrogen Life Science (Paisley, UK). The synthetic $A\beta_{1\text{-}40}$ peptide was from Bachem (Bubendorf, Switzerland). Polyvinylidene difluoride (PVDF) membrane, goat alkaline phosphatase-linked anti-rabbit and anti-mouse secondary antibodies, and the Enhanced chemifluorescence (ECF) reagent were acquired from Amersham Pharmacia Biotech (Buckinghamshire, UK). Mouse monoclonal antibody against glyceraldehyde-3-phosphate dehydrogenase (GAPDH) was from Chemicon International Inc. (Temecula, CA, USA). Bio-Rad protein dye assay reagent and acrylamide were purchased from Bio-Rad (Hercules, CA, USA). Collagen was obtained from Advanced BioMatrix, Inc. (San Diego, CA, USA). Trypsin-ethylenediaminetetraacetic acid (EDTA) solution, protease inhibitors (leupeptin, pepstatin A, chymostatin, and aprotinin), recombinant human basic fibroblast growth factor (bFGF), coelenterazine WT and N, glucose, ionomycin, bovine serum albumin (BSA), Tris-HCl, Triton X-100, Na-deoxycholate, sodium dodecyl sulfate (SDS), NaCl, KCl, $MgCl_2$, $CaCl_2$, orthovanadate, NaF, hydroxyethyl piperazineethanesulfonic acid (HEPES)-Na, $MgCl_2$, EDTA, EGTA, phenylmethylsulfonyl fluoride (PMSF), dithiothreitol (DTT), NaOH, H_3PO_4, NaH_2PO_4, Na_3PO_4, $MgSO_4$, adenosine triphosphate (ATP), oxidized glutathione (GSSG) and GSH, O-phthaldehyde (OPT), N-ethylmaleimide (NEM), and the rabbit polyclonal anti-actin and mouse monoclonal anti-β-tubulin antibodies were obtained from Sigma Chemical Co. (St. Louis, MO, USA). The ProteoExtract® Subcellular Proteome Extraction Kit was purchased from Calbiochem (Darmstadt, Germany). 2′,7′-Dichlorodihydrofluorescein diacetate ($DCFH_2$-DA) was obtained from Molecular Probes (Leiden, The Netherlands). The mouse monoclonal anti-SERCA2, anti-HIF-1α, and anti-TATA-box binding protein (TBP) and the rabbit polyclonal anti-VDAC, anti-Nrf2, and anti-glutathione reductase (GRd) antibodies were acquired from Abcam plc (Cambridge, UK). The rabbit polyclonal anti-IP3R was from BD Biosciences (Franklin Lakes, NJ, USA). The rabbit polyclonal anti-vascular endothelial growth factor (VEGF) and anti-glucose transporter (GLUT)1 antibodies were from Merck KGaA (Darmstadt, Germany). The goat horseradish peroxidase conjugated anti-rabbit and anti-mouse secondary antibodies, the donkey alkaline phosphatase conjugated anti-goat secondary antibody, the rabbit polyclonal anti-stromal interaction molecule (STIM)1 and anti-Orai1 antibodies, and the goat polyclonal anti-peroxisome proliferator-activated receptor gamma, coactivator 1 alpha (PGC1α) antibody were purchased from Santa Cruz Biotechnology Inc. (Santa Cruz, CA, USA).

Culture and Treatments of Rat Brain Endothelial Cells

The rat brain RBE4 cell line, provided by Dr. Jon Holy (University of Minnesota, Duluth, USA), was cultured as described previously [33]. RBE4 cells plated on collagen-coated multiwell plates were treated during 3–24 h with synthetic $A\beta_{1\text{-}40}$ at a concentration of 2.5 μM, which was found to be enriched in high molecular weight oligomers with more than 50 kDa that are toxic [33] and induce a time-dependent intracellular accumulation of Aβ in this cell line [49]. Thereafter, levels of hydroperoxides, GSH and GSSG, and also of several signaling proteins were measured. Alternatively, cells plated in plastic coverslips coated with collagen at a similar density were transfected with aequorin complementary DNA (cDNA) and treated with $A\beta_{1\text{-}40}$ during 1–24 h for Ca^{2+} measurements.

Rat Brain Endothelial Cell Transfection

RBE4 cells were transfected with chimeric aequorins targeted to the ER (erAEQmut), cytosol (cytAEQ), and mitochondria (mtAEQmut) using the calcium phosphate method. "AEQ" refers to wild-type aequorin, and "AEQmut" refers to a low-affinity D119A mutant of aequorin. Briefly, 1 h before the transfection, the cell culture medium was replaced by fresh medium and then the transfection solution (40 μg DNA/ml and 125 mM $CaCl_2$ plus, in millimolar, 140 NaCl, 25 HEPES, and 0.75 Na_2HPO_4, pH 7.12) was added. After 16 h, cells were washed with phosphate buffered saline (PBS), culture medium was refreshed, and aequorin measurements were performed 32 h later.

Aequorin Measurements

The analysis of erAEQmut was performed as previously described [50].

Concerning the experiments with cytAEQ and mtAEQmut, RBE4 cells were incubated for 90 min with 25 μM coelenterazine WT, which was added directly to culture medium, and aequorin measurements were performed in Ca^{2+}-supplemented medium in the presence of 100 μM ATP to induce the release of Ca^{2+} from ER [50].

The output of the discriminator was captured by a Thorn EMI photon-counting board and stored in an IBM-compatible computer for further analyses. The aequorin luminescence data were calibrated offline into $[Ca^{2+}]$ values, which were expressed in micromolar, using a computer algorithm based on the Ca^{2+} response curve of wild-type and mutant aequorins [50].

The maximal retention of Ca^{2+} in the ER and the rate of Ca^{2+} uptake into this organelle were calculated upon addition of 1 mM $CaCl_2$ in erAEQmut-expressing cells and were

expressed in micromolar and micromolar per second, respectively. Moreover, the maximum retention of Ca^{2+} in the mitochondria or cytosol was calculated upon addition of ATP in mtAEQmut- or cytAEQ-expressing cells.

Protein Analysis by Western Blot

The levels of proteins involved in Ca^{2+} homeostasis and oxidative stress were analyzed by immunoblotting using cellular extracts obtained from treated or untreated RBE4 cells [33, 51]. Additionally, the nuclear Nrf2 and HIF-1α protein levels were evaluated by immunoblotting using nuclear fractions obtained with the ProteoExtract® Subcellular Proteome Extraction Kit according to the manufacturer's instruction. The protein content was measured using the Bio-Rad protein dye assay reagent.

Total extracts containing 10 μg protein (for SERCA2, IP_3R, VDAC, STIM1, and Orai1) or 30 μg protein (for GRd, PGC1α, VEGF, and GLUT1), or nuclear fractions containing 30 μg protein (for Nrf2 and HIF-1α), were separated by electrophoresis and transferred to PVDF membranes [33]. The membranes were incubated overnight at 4ºC with primary antibodies, diluted in TBS-T: SECA2 (1:500), total IP_3R (1:500), total VDAC (1:3,000), STIM1 (1:1,000), Orai1 (1:1,000), Nrf2 (1:1,000), GRd (1:2,000), PGC1α (1:500), HIF-1α (1:500), VEGF (1:500), or GLUT1 (1:500). Control of protein loading was performed using primary antibodies against β-tubulin (1:3,000), actin (1:5,000), or GAPDH (1:10,000) for total cellular extracts and a primary antibody against TBP (1:2,000) for nuclear extracts. After washing, membranes were incubated for 1 h at RT with an alkaline phosphatase or horseradish peroxidase-conjugated secondary anti-mouse or anti-rabbit or anti-goat antibody (1:20,000). Bands of immunoreactive proteins were visualized after membrane incubation with ECF or ECL reagents during approximately 5 min, and densities of protein bands were calculated using the WCIF ImageJ program (Wayne Rasband, Research Services Branch, National Institute of Mental Health, Bethesda, MD, USA). The ratios between SERCA2, total IP_3R, or total VDAC and β-tubulin; the ratios between STIM1 or Orai1 and actin; the ratio between nuclear HIF-1α or nuclear Nrf2 and TBP; and the ratios between GRd, PGC1α, VEGF, or GLUT1 and GAPDH were calculated, and results were expressed relatively to control values.

Quantification of Intracellular Reactive Oxygen Species

The oxidant-sensitive dye $DCFH_2$-DA was used to evaluate changes in intracellular hydroperoxide levels [52, 53], as previously described [44].

Measurement of Reduced and Oxidized Glutathione Intracellular Levels

The ratio between reduced and oxidized glutathione (GSH/GSSG) is a good indicator of oxidative stress in cells. After treatments, endothelial cells were washed two times with PBS; lysed at 4ºC in 15 mM Tris pH 7.4 supplemented with 0.1 mM PMSF, 2 mM DTT, and 1:1,000 of a protease inhibitor cocktail (1 μg/ml leupeptin, pepstatin A, chymostatin, and antipain); and the levels of GSH and GSSG were evaluated in a microplate reader (SpectraMax Gemini EM fluorocytometer) [54]. The results were determined in microgram GSH or GSSG per microgram protein, and the ratio between GSSG and GSH was calculated and expressed relatively to the control.

Data Analysis

Data were expressed as means±SEM of measurements performed in duplicate, from at least three independent experiments. Statistical significance analysis was determined using one-way ANOVA followed by Dunnett's post hoc tests or using Student's *t* test in the GraphPad Prism Software (San Diego, CA, USA). The differences were considered significant for P values <0.05.

Results

Ca^{2+} Homeostasis in Brain Endothelial Cells Is Deregulated by $A\beta_{1\text{-}40}$

Changes in intracellular Ca^{2+} homeostasis were investigated in RBE4 cells after treatment for 1–24 h with 2.5 μM $A\beta_{1\text{-}40}$, a concentration that was previously demonstrated to induce a significant decrease in RBE4 cell survival [33]. For that purpose, aequorin probes targeted to different subcellular compartments, namely, mitochondrial matrix, ER lumen, or cytosol, were used [50]. The response of the ER to reestablish Ca^{2+} levels after the removal of intracellular Ca^{2+} with EGTA and ionomycin was significantly reduced by $A\beta_{1\text{-}40}$ with a maximal decrease observed 3 and 6 h after treatment (Fig. 1a–c). Moreover, the rate of ER Ca^{2+} refill also decreased with minimum values reached at 6 h (Fig. 1b and d). In addition, a time-dependent increase in basal $[Ca^{2+}]_{mit}$ was determined during $A\beta_{1\text{-}40}$ exposure, which reached statistical significance at 6 and 12 h compared to untreated cells (Fig. 2b and c). ATP-induced Ca^{2+} release from ER increased significantly the concentration of Ca^{2+} in mitochondria ($[Ca^{2+}]_{mit}$) (Fig. 2a and d) and in the cytosol ($[Ca^{2+}]_{cyt}$) (Fig. 3a and c) in cells treated during 1 or 3 h with $A\beta_{1\text{-}40}$, which recovered after that (Figs. 2 and 3).

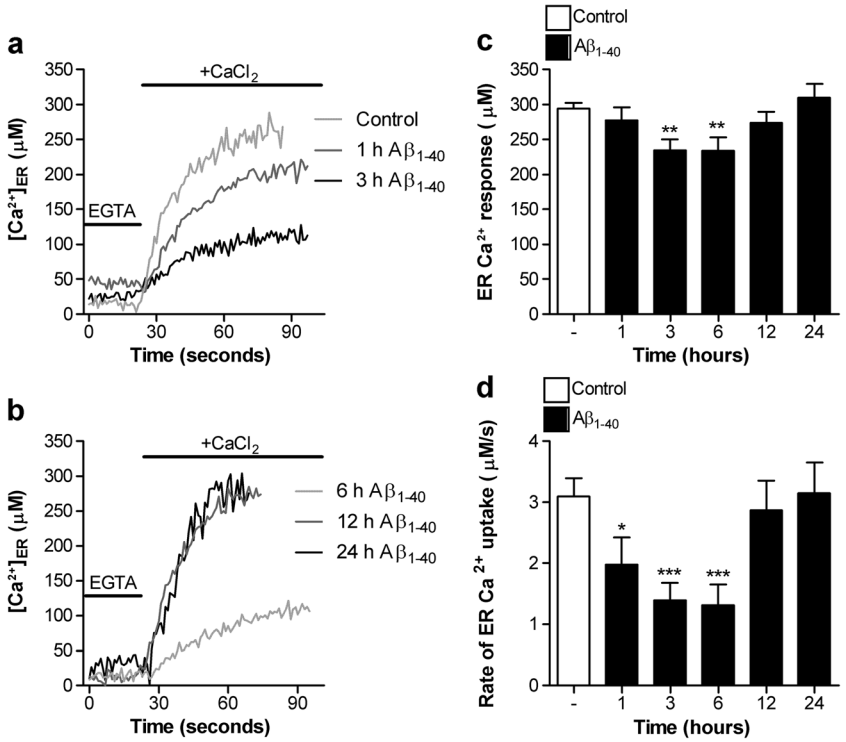

Fig. 1 $A\beta_{1-40}$ deregulates endoplasmic reticulum (*ER*) Ca^{2+} homeostasis in brain endothelial cells. RBE4 cells transfected with aequorin chimera targeted to ER lumen were treated with $A\beta_{1-40}$ (2.5 μM) for 1, 3, 6, 12, or 24 h. For the analysis of the ability of the ER to store Ca^{2+} (**a** and **b**), these ions were first removed from the cytosol and intracellular stores with a Ca^{2+} chelator and were then replaced through the addition of 1 mM $CaCl_2$. The ER Ca^{2+} response (**c**) corresponds to the maximum peak in $[Ca^{2+}]_{ER}$ after Ca^{2+} replacement, and the rate of ER Ca^{2+} uptake (**d**) corresponds to the slope of the regression line calculated after Ca^{2+} addition. All traces correspond to single representative experiments (**a** and **b**), and *graphic bars* represent the means±SEM of at least 12 independent experiments. *$p<0.05$, **$p<0.01$, and ***$p<0.001$ significantly different from control

Fig. 2 $A\beta_{1-40}$ deregulates mitochondrial Ca^{2+} homeostasis in brain endothelial cells. RBE4 cells transfected with aequorin chimera targeted to mitochondrial matrix were treated with $A\beta_{1-40}$ (2.5 μM) for 1, 3, 6, 12, or 24 h. Cells were stimulated with ATP (100 μM) and basal $[Ca^{2+}]_{mit}$ (**a**, **b**, and **c**), corresponding to $[Ca^{2+}]_{mit}$ before the addition of ATP, and mitochondrial Ca^{2+} responses (**a**, **b**, and **d**), corresponding to the maximum peak after the addition of ATP, were analyzed. All traces correspond to single representative experiments (**a** and **b**), and *graphic bars* represent the means±SEM of at least eight independent experiments. *$p<0.05$ significantly different from control

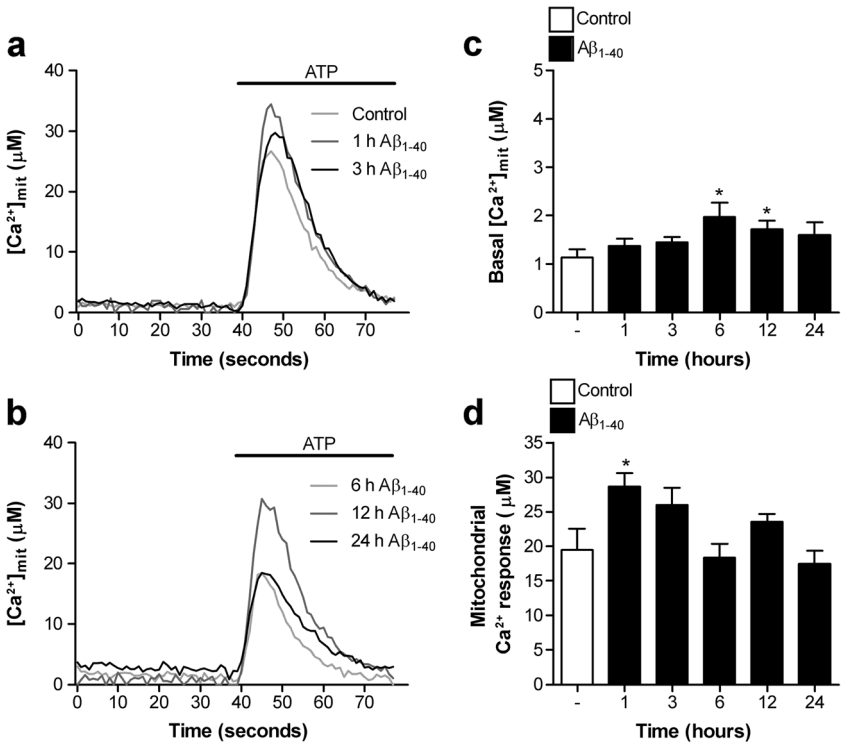

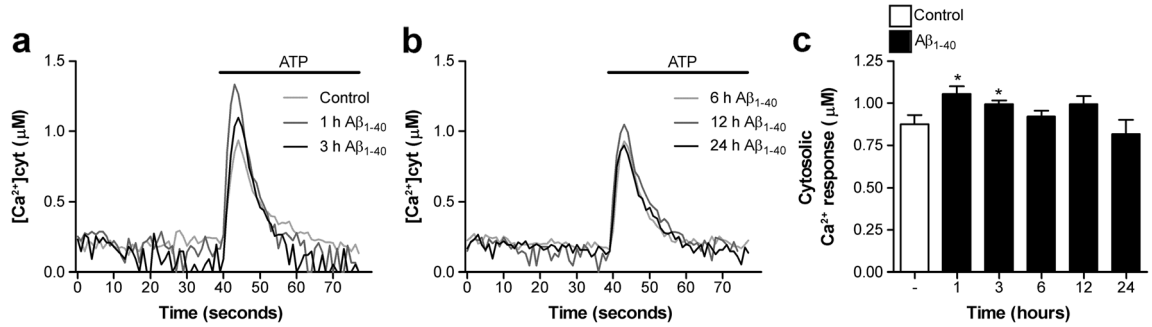

Fig. 3 $A\beta_{1\text{-}40}$ deregulates cytosolic Ca^{2+} homeostasis in brain endothelial cells. RBE4 cells transfected with aequorin chimera that localizes in the cytosol were treated with $A\beta_{1\text{-}40}$ (2.5 μM) for 1, 3, 6, 12, or 24 h. Cells were stimulated with ATP (100 μM), and cytosolic Ca^{2+} responses corresponding to the maximum peak after the addition of ATP were analyzed (**c**). All traces correspond to single representative experiments (**a** and **b**), and *graphic bar* represents the means±SEM of at least eight independent experiments. *$p<0.05$ significantly different from control

$A\beta_{1\text{-}40}$ Affects the Levels of Proteins That Regulate Ca^{2+} Homeostasis in Brain Endothelial Cells

Since Ca^{2+} homeostasis was altered in RBE4 cells treated with $A\beta_{1\text{-}40}$, the protein levels of regulators of Ca^{2+} homeostasis were analyzed by Western blotting (WB). The levels of SERCA2, a Ca^{2+}-ATPase responsible for Ca^{2+} transfer from the cytosol to the ER lumen, significantly increased after 3 h of $A\beta_{1\text{-}40}$ treatment and decreased after that until a significant decrease was measured at 24 h (Fig. 4a and b). WB analysis revealed a time-dependent reduction on the levels of an ER membrane-resident receptor involved in Ca^{2+} release, the IP_3R, which becomes significant upon 24 h of $A\beta_{1\text{-}40}$ incubation (Fig. 4a and c). The protein levels of VDAC, which is located in the outer mitochondrial membrane and is an important regulator of Ca^{2+} fluxes between the ER and the mitochondria, also decreased in a time-dependent manner, and the decrease was shown to be statistically significant at 12 and 24 h of incubation with $A\beta_{1\text{-}40}$ (Fig. 4a and d). Similarly, the protein levels of STIM1 and Orai1, that regulate the entry of Ca^{2+} at the plasma membrane level after the depletion of ER Ca^{2+}, significantly decreased in cells treated with $A\beta_{1\text{-}40}$ for more than 12 h (Fig. 4a, e, and f).

Brain Endothelial Cells Undergo Changes in Redox Homeostasis When Exposed to $A\beta_{1\text{-}40}$

In order to investigate the redox status under conditions of perturbed Ca^{2+} homeostasis triggered by $A\beta_{1\text{-}40}$ in brain endothelial cells, a time-dependent analysis of the levels of intracellular hydroperoxides and of the GSH/GSSG ratio was performed in control versus $A\beta_{1\text{-}40}$-treated RBE4 cells. At 3 h of treatment, the levels of intracellular hydroperoxides measured with $DCFH_2$-DA reached a maximum then decreased, and no significant differences between controls and treated cells were detected at 24 h (Fig. 5a). The GSH levels decreased until 6 h of $A\beta_{1\text{-}40}$ incubation and returned to control levels at 24 h (Fig. 5b), and the GSSG levels significantly increased during the 3–24-h period of $A\beta_{1\text{-}40}$ treatment (Fig. 5c). Under these conditions, the ratio between GSH and GSSG significantly decreased in $A\beta_{1\text{-}40}$-treated cells with a maximum reduction at 6 h (Fig. 5d).

$A\beta_{1\text{-}40}$ Activates Oxidative Stress Responses in Brain Endothelial Cells

The protein levels of mediators of the cellular response to oxidative stress, namely, the transcription factors Nrf2 and HIF-1α, were analyzed in RBE4 cells treated during 3, 6, 12, or 24 h with $A\beta_{1\text{-}40}$ by immunoblotting. Nrf2 is known to increase the expression of PGC1α and several antioxidant enzymes involved in GSH metabolism including GRd, and HIF-1α upregulates genes such as VEGF and the glucose transporter GLUT1. Nrf2 nuclear levels increased until 12 h of $A\beta_{1\text{-}40}$ exposure and then returned to control values (Fig. 6a and b). In addition, the levels of GRd increased significantly at 12 and 24 h of $A\beta_{1\text{-}40}$ treatment, and PGC1α was upregulated after 6 h of $A\beta_{1\text{-}40}$ exposure (Fig. 6a, c, and d). A significant time-dependent increase in HIF-1α levels was detected in the nucleus upon incubation with $A\beta_{1\text{-}40}$ (Fig. 6a and e). Concomitantly or following this increase of nuclear HIF-1α, the levels of VEGF and GLUT1 increased in $A\beta_{1\text{-}40}$-treated cells (Fig. 6a, f, and g).

Discussion

Endothelial dysfunction induced by Aβ accumulated around brain microvascular endothelial cells has been implicated in the cerebrovascular alterations that occur in AD and has been shown to potentiate neuronal degeneration and cognitive impairment [55–57]. In this study, it was demonstrated that concentrations of $A\beta_{1\text{-}40}$ that were previously found to induce endothelial cells' death cause time-dependent alterations in Ca^{2+} and redox homeostasis in these brain cells.

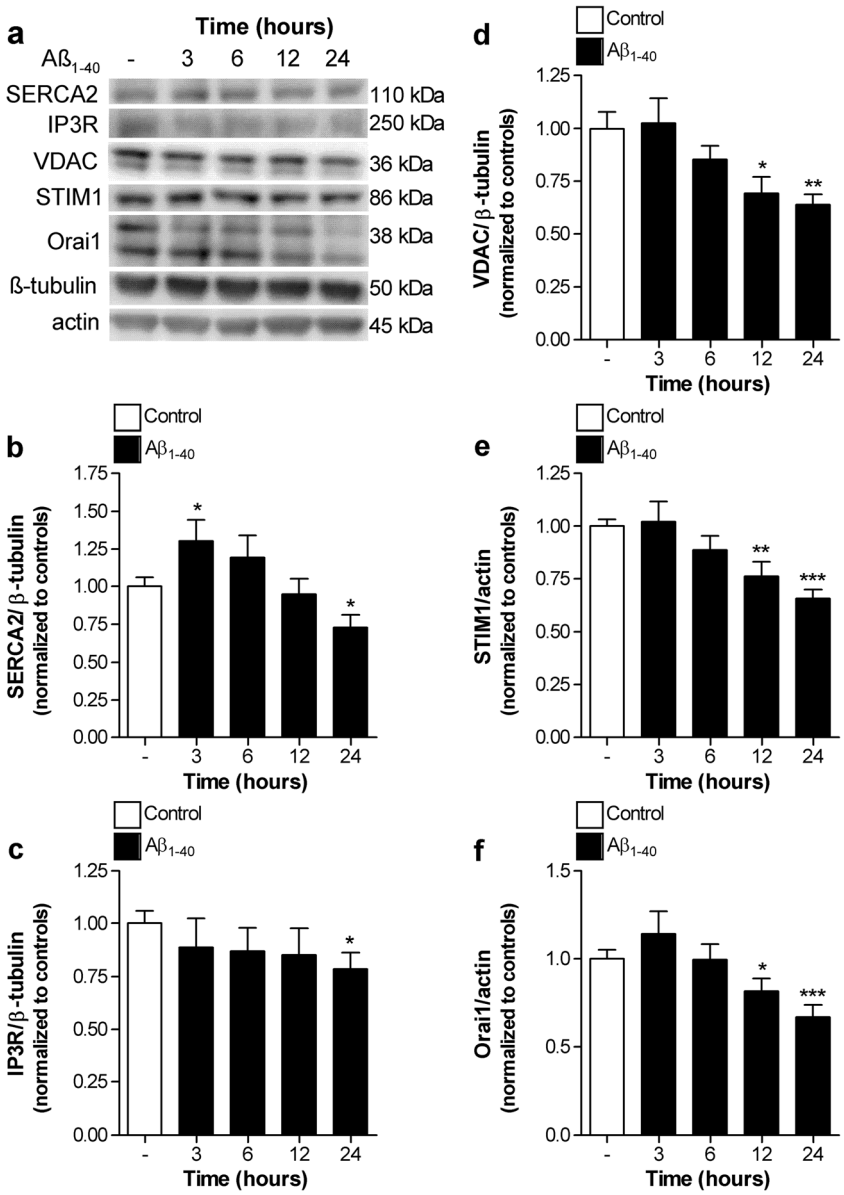

Fig. 4 Levels of proteins involved in the regulation of Ca^{2+} homeostasis are altered by $A\beta_{1\text{-}40}$ in brain endothelial cells. Protein levels of SERCA2 (**a** and **b**), total IP_3Rs (**a** and **c**), total VDACs (**a** and **d**), STIM1 (**a** and **e**), and Orai1 (**a** and **f**) were quantified by immunoblotting in cellular extracts obtained from RBE4 cells treated with $A\beta_{1\text{-}40}$ (2.5 μM) for 3, 6, 12, or 24 h. Anti-β-tubulin or anti-actin antibodies were applied as protein loading controls and used to normalize the levels of proteins of interest. The results were calculated relatively to control values and represent the means±SEM of at least eight independent experiments. *$p<0.05$, **$p<0.01$, and ***$p<0.001$ significantly different from untreated cells

The precise concentration that Aβ can reach in the parenchyma or microvessels of human AD brain is not known. However, the study of Miao and collaborators in brain microvessels isolated from AD transgenic mice demonstrates that Aβ concentration is above 400 ng/mg total protein and is higher than that determined in the brain parenchyma [12]. Nevertheless, the concentration of Aβ along microvessels is variable, and quantifications, which are usually performed in homogenates, correspond to an average value and do not mirror the concentration in each point of microvessels. Therefore, the concentration of Aβ to which some endothelial cells are exposed can be very high and similar to that used in the present study. Finally, some reports describe the use of higher concentrations, namely, 50 to 200 μM $A\beta_{1\text{-}42}$, the less concentrated Aβ form in brain parenchyma and microvessels [12], to treat vascular cells [58, 59]. On the other hand, the $A\beta_{1\text{-}40}$ used is enriched in species with more than 50 kDa, which were demonstrated to be highly toxic [60–64] and that induce the intracellular accumulation of Aβ in brain endothelial cells [33, 49].

Previously, we have shown that $A\beta_{1\text{-}40}$ depletes ER Ca^{2+} stores and induces a sustained rise of $[Ca^{2+}]_{cyt}$ [33]. In the present study, we showed that $A\beta_{1\text{-}40}$ also diminishes the capacity to restore Ca^{2+} levels in the ER lumen upon Ca^{2+} depletion and found that $A\beta_{1\text{-}40}$ interferes with the cytosolic and mitochondrial responses to ER Ca^{2+} depletion triggered by ATP. These changes were associated with alterations in the levels of proteins involved in Ca^{2+} homeostasis in the ER, plasma membrane, and mitochondria. The early increase observed in $A\beta_{1\text{-}40}$-treated cells in the levels of SERCA2, which

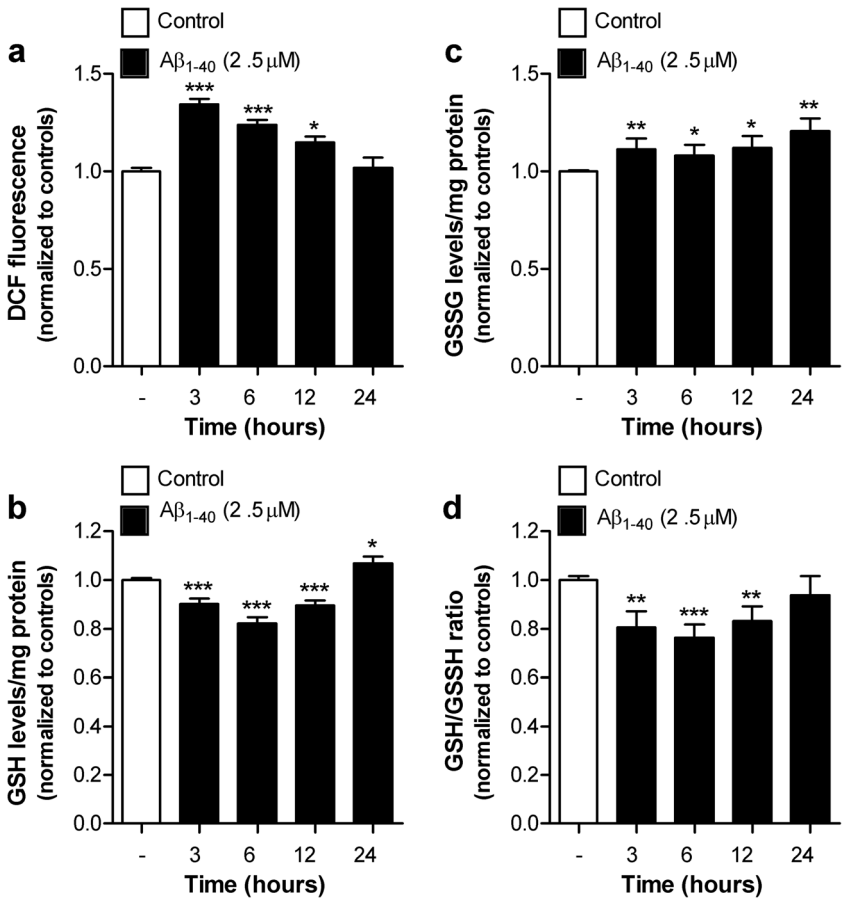

Fig. 5 $A\beta_{1\text{-}40}$ affects redox homeostasis in brain endothelial cells. After treatment for 3, 6, 12, or 24 h with $A\beta_{1\text{-}40}$ (2.5 μM), DCF fluorescence was analyzed in RBE4 cells in order to analyze the levels of ROS (**a**). In cellular extracts obtained from control and treated cells, GSH (**b**) and GSSG (**c**) levels were quantified and the ratio GSH/GSSG was calculated (**d**). Data were normalized to control, and the results represent the means±SEM of at least five independent experiments performed in duplicate. *$p<0.05$, **$p<0.01$, and ***$p<0.001$ significantly different from control

is responsible for ER Ca^{2+} load, can represent a compensatory mechanism to avoid ER Ca^{2+} depletion. The rise in $[Ca^{2+}]_{cyt}$ that occurs in $A\beta_{1\text{-}40}$-treated endothelial cells is probably responsible for the reduction in the levels of the SOCE components STIM1 and Orai1, which become unable to compensate ER Ca^{2+} depletion in $A\beta_{1\text{-}40}$-treated cells. In addition, this decrease can promote Aβ generation and toxicity since overexpression of STIM1 and Orai1 was shown to significantly reduce Aβ secretion [65]. The release of ER Ca^{2+} by IP_3Rs and consequent mitochondrial Ca^{2+} overload was demonstrated in several apoptosis paradigms [66–68]. Previous studies in cultured rat cortical neurons demonstrated that $A\beta_{1\text{-}40}$ and $A\beta_{1\text{-}42}$ increase the release of Ca^{2+} from ER through IP_3Rs and also by RyRs, leading to mitochondrial depolarization and release of pro-apoptotic factors [32, 61, 69]. Accordingly, inhibition of ER Ca^{2+} release was shown to reduce Aβ levels and to preserve synaptic function in hippocampal slices from an AD mice model [32, 61, 69]. Mitochondrial VDAC is physically linked to the ER-resident IP_3Rs through GRP75 and is involved in Ca^{2+} communication between the ER and mitochondria [68, 70, 71]. Recently, increased IP_3R and VDAC levels were found in primary hippocampal neurons treated for 8 and 48 h with nanomolar $A\beta_{1\text{-}40}$ and $A\beta_{1\text{-}42}$, as well as an increase in the number of ER-mitochondria contact points and $[Ca^{2+}]_{mit}$ [28]. Here, the total levels of VDAC and IP_3R decreased after 24-h exposure of endothelial cells to higher $A\beta_{1\text{-}40}$ doses (micromolar range), and consequently, the Ca^{2+} signals between ER and mitochondria were diminished, possibly in an attempt to overcome excessive ER-to-mitochondria Ca^{2+} transfer and mitochondrial Ca^{2+} overload and to prevent activation of mitochondria-mediated apoptotic cell death pathways. Although $[Ca^{2+}]_{mit}$ returned to values similar to control, Aβ-induced endothelial cell death was not avoided since it was previously shown that $A\beta_{1\text{-}40}$ induces mitochondria-dependent apoptosis in vascular endothelial cells through the release of cytochrome c, activation of caspase-9 and caspase-3, and translocation of the apoptosis-inducing factor from mitochondria to the nucleus [33, 72–74]. Furthermore, the inhibition of ER Ca^{2+} release is able to prevent mitochondrial membrane depolarization induced by $A\beta_{1\text{-}40}$ [33].

When $[Ca^{2+}]_{ER}$ decreases, the ER-resident STIM protein co-localizes with the plasma membrane-Orai protein, promoting the entry of Ca^{2+} into the cell through SOCE. The increase in intracellular Ca^{2+} levels in brain endothelial cells after the activation of SOCE was shown to trigger the reorganization of the cytoskeleton, which disrupts the endothelial cell barrier and increases blood-brain barrier permeability [75] that is

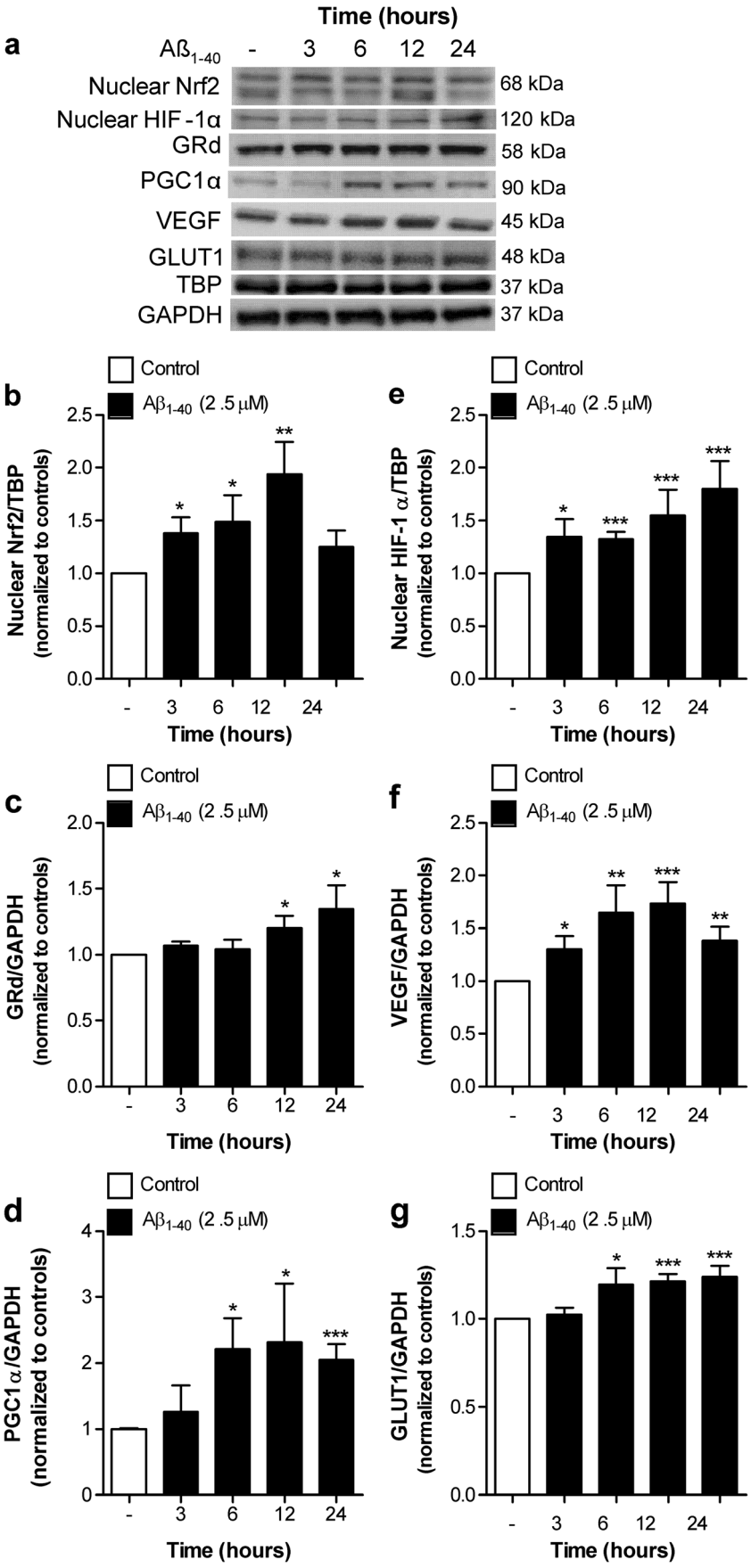

Fig. 6 $A\beta_{1\text{-}40}$ activates an oxidative stress response in brain endothelial cells. RBE4 cells were treated with $A\beta_{1\text{-}40}$ (2.5 μM) for 3, 6, 12, or 24 h, and the protein levels of Nrf2 (**a** and **b**), GRd (**a** and **c**), PGC1α (**a** and **d**), HIF-1α (**a** and **e**), VEGF (**a** and **f**), and GLUT1 (**a** and **g**) were quantified by immunoblotting using total cell lysates or nuclear extracts. Anti-GAPDH and anti-TATA box protein (TBP) antibodies were applied as protein loading controls in total or nuclear extracts, respectively, and used to normalize the levels of the proteins of interest. The results were calculated relatively to control values and represent the means±SEM of at least eight independent experiments. *$p<0.05$, **$p<0.01$, and ***$p<0.001$ significantly different from control

found in AD patients [76]. During physiological conditions, Ca^{2+} from SOCE is rapidly captured by adjacent mitochondria to maintain the $[Ca^{2+}]_{cyt}$ at low levels, allowing the entry of more Ca^{2+}. Mitochondrial Ca^{2+} is then exported to the cytosol through the Na^{+}/Ca^{2+}-exchanger in regions close to the ER and captured by SERCA to reestablish the $[Ca^{2+}]_{ER}$ [77]. However, oxidants can decrease the activity of the Na^{+}/Ca^{2+}-exchanger, plasma membrane Ca^{2+}-ATPases, and SERCA and thus impair the reestablishment of $[Ca^{2+}]_{ER}$, causing prolonged mitochondrial Ca^{2+} elevation [39, 78]. This is in accordance with the present results that show a temporal correlation between oxidative stress, ER Ca^{2+} entry, and $[Ca^{2+}]_{mit}$. Because the ER has several Ca^{2+}-dependent chaperones, the reduction of $[Ca^{2+}]_{ER}$ can induce ER stress as previously demonstrated in RBE4 cells and other cell types treated with $A\beta_{1\text{-}40}$ and also in AD animal models and AD patients [33, 79, 80].

Stimulation of RBE4 cells with ATP activates metabotropic ATP receptors in the plasma membrane leading to IP_3 generation that activates IP_3Rs in the ER and releases Ca^{2+} from this organelle, which in turn increases cytosolic and mitochondrial $[Ca^{2+}]$. However, we cannot exclude the contribution of activated ionotropic ATP receptors since, like the metabotropic receptors, they are abundant in brain microvascular endothelial cells [81].

The alterations in Ca^{2+} homeostasis, namely, the increase in $[Ca^{2+}]_{mit}$ in brain endothelial cells, can increase ROS production [35, 42]. Numerous studies establish a close relationship between oxidative stress and endothelial dysfunction [48, 82]. Furthermore, it was previously demonstrated in cortical neurons that the release of Ca^{2+} from the ER induced by $A\beta_{1\text{-}40}$ increases the levels of intracellular ROS [83]. Moreover, $A\beta_{1\text{-}40}$ was shown to increase the levels of ROS in microvascular endothelial cells isolated from rat brain [84]. The decrease in ER Ca^{2+} content causes ER stress and consequently upregulates GADD153 (growth arrest and DNA damage-inducible protein 153)/CHOP, a pro-apoptotic transcription factor that activates GADD34, which in turn increases ROS generation [85]. Accordingly, the time-dependent change in GADD153/CHOP levels that was recently observed in RBE4 cells treated with $A\beta_{1\text{-}40}$ [33] correlates with the alterations that were now found in ROS levels. Moreover, ER stress and ATP depletion resulting from increased $[Ca^{2+}]_{mit}$ in $A\beta_{1\text{-}40}$-treated RBE4 cells, together with SERCA2 inhibition, can block general protein translation and synthesis [31, 33, 86, 87]. This contributes to a general decrease in protein levels and in a delay in cellular responses dependent of protein synthesis particularly those that follow the secretory pathway, such as membrane Ca^{2+} channels.

In addition to a time-dependent increase in ROS levels, a significant depletion of the antioxidant GSH in brain endothelial cells treated with $A\beta_{1\text{-}40}$ that was accompanied by an increase in GSSG was also detected, leading to the reduction of the GSH/GSSG ratio. The recovery of GSH levels at 24 h can be due to antioxidant responses induced by the activation of protein kinase RNA-like endoplasmic reticulum kinase (PERK) and subsequent upregulation of the activating transcription factor 4 and Nrf2 in order to restore cellular homeostasis [33, 88]. Both transcription factors are involved in antioxidant responses, leading to expression of proteins involved in GSH biosynthesis [88–90]. Accordingly, the levels of glutathione reductase, which converts GSSG in GSH, were upregulated by prolonged exposure to $A\beta_{1\text{-}40}$ and might underlie the recovery of GSH levels in $A\beta_{1\text{-}40}$-treated cells. ROS can also activate Nrf2 in vascular endothelial cells, and the neutralization of ROS suppresses Nrf2 activation [91]. Therefore, the restoration of Nrf2 levels at 24 h in $A\beta_{1\text{-}40}$-treated cells can result from the increase of antioxidant defenses that seems to compensate the increase of ROS and also because ER stress is normalized to values similar to those of untreated cells [33]. Another transcription factor that can be translocated to the nucleus in the presence of ROS is HIF-1α [92]. Under normoxic conditions, HIF-1α in the cytosol is hydroxylated by oxygen-dependent prolyl hydrolases that leads to polyubiquitination and rapid degradation by the proteasome. Under low levels of oxygen, HIF-1α is not hydroxylated and consequently is translocated to the nucleus, dimerizes with the constitutively expressed HIF-1β, and regulates hypoxia-related genes [93]. The increased ROS production in mitochondria during hypoxia is also necessary and sufficient to activate HIF-1α [94, 95]. Furthermore, an increase in ROS production and oxidative stress was found during hypoxia in different cell types [96, 97]. Here, the levels of HIF-1α in the nucleus increased in $A\beta_{1\text{-}40}$-treated cells, which was correlated with changes in GSSG levels (an oxidative stress maker) and with the previously reported proteasomal inhibition [49, 98, 99]. In this way, the degradation of HIF-1α in the proteasome diminishes and contributes to the translocation of HIF-1α to the nucleus where it induces the expression of cell survival and angiogenic genes, such as VEGF, and glucose transporters, namely, GLUT1 and GLUT3 [93, 100], as observed in brain endothelial cells treated with $A\beta_{1\text{-}40}$.

Conclusion

Exposure of rat brain endothelial cells to a toxic dose of $A\beta_{1\text{-}40}$ deregulates Ca^{2+} and redox homeostasis, which is accompanied by the induction of compensatory responses. However, these mechanisms are not able to counteract the deleterious effects of $A\beta_{1\text{-}40}$, and endothelial cells die by apoptosis, as previously demonstrated.

Acknowledgments The authors are grateful to Dr. Jon Holy (University of Minnesota, Duluth, USA) for the generous gift of RBE4 cells. This work was supported by "Fundação para a Ciência e a Tecnologia",

Portugal (the project PEst-C/SAU/LA0001/2011 and the Ph.D. fellowship attributed to AC Fonseca: SFRH/BD/47573/2008); the Italian Association for Cancer Research (AIRC); Telethon (GGP11139B); local funds from the University of Ferrara; the Italian Ministry of Education, University and Research (COFIN, FIRB, and Futuro in Ricerca); and the Italian Ministry of Health.

Conflict of Interest The authors declare that they have no conflict of interest.

References

1. Carvalho C, Machado N, Mota PC, Correia SC, Cardoso S, Santos RX, Santos MS, Oliveira CR, Moreira PI (2013) Type 2 diabetic and Alzheimer's disease mice present similar behavioral, cognitive, and vascular anomalies. J Alzheimers Dis 35(3):623–635
2. Karran E, Mercken M, De Strooper B (2011) The amyloid cascade hypothesis for Alzheimer's disease: an appraisal for the development of therapeutics. Nat Rev Drug Discov 10(9):698–712
3. Zlokovic BV (2011) Neurovascular pathways to neurodegeneration in Alzheimer's disease and other disorders. Nat Rev 12(12):723–738
4. Dorr A, Sahota B, Chinta LV, Brown ME, Lai AY, Ma K, Hawkes CA, McLaurin J, Stefanovic B (2012) Amyloid-beta-dependent compromise of microvascular structure and function in a model of Alzheimer's disease. Brain 135(Pt 10):3039–3050
5. Pluta R, Jablonski M, Ulamek-Koziol M, Kocki J, Brzozowska J, Januszewski S, Furmaga-Jablonska W, Bogucka-Kocka A, Maciejewski R, Czuczwar SJ (2013) Sporadic Alzheimer's disease begins as episodes of brain ischemia and ischemically dysregulated Alzheimer's disease genes. Mol Neurobiol 48(3):500–515
6. Sagare AP, Bell RD, Zlokovic BV (2012) Neurovascular dysfunction and faulty amyloid beta-peptide clearance in Alzheimer disease. Cold Spring Harb Perspect Med 2(10)
7. Yamada K, Yabuki C, Seubert P, Schenk D, Hori Y, Ohtsuki S, Terasaki T, Hashimoto T, Iwatsubo T (2009) Abeta immunotherapy: intracerebral sequestration of Abeta by an anti-Abeta monoclonal antibody 266 with high affinity to soluble Abeta. J Neurosci 29(36):11393–11398
8. Holmes C, Boche D, Wilkinson D, Yadegarfar G, Hopkins V, Bayer A, Jones RW, Bullock R, Love S, Neal JW, Zotova E, Nicoll JA (2008) Long-term effects of Abeta42 immunisation in Alzheimer's disease: follow-up of a randomised, placebo-controlled phase I trial. Lancet 372(9634):216–223
9. Ito S, Ohtsuki S, Murata S, Katsukura Y, Suzuki H, Funaki M, Tachikawa M, Terasaki T (2014) Involvement of insulin-degrading enzyme in insulin- and atrial natriuretic peptide-sensitive internalization of amyloid-beta peptide in mouse brain capillary endothelial cells. J Alzheimers Dis 38(1):185–200
10. Park MH, Lee JK, Choi S, Ahn J, Jin HK, Park JS, Bae JS (2013) Recombinant soluble neprilysin reduces amyloid-beta accumulation and improves memory impairment in Alzheimer's disease mice. Brain Res 1529:113–124
11. Attems J, Yamaguchi H, Saido TC, Thal DR (2010) Capillary CAA and perivascular Abeta-deposition: two distinct features of Alzheimer's disease pathology. J Neurol Sci 299(1–2):155–162
12. Miao J, Xu F, Davis J, Otte-Holler I, Verbeek MM, Van Nostrand WE (2005) Cerebral microvascular amyloid beta protein deposition induces vascular degeneration and neuroinflammation in transgenic mice expressing human vasculotropic mutant amyloid beta precursor protein. Am J Pathol 167(2):505–515
13. Hartz AM, Bauer B, Soldner EL, Wolf A, Boy S, Backhaus R, Mihaljevic I, Bogdahn U, Klunemann HH, Schuierer G, Schlachetzki F (2012) Amyloid-beta contributes to blood-brain barrier leakage in transgenic human amyloid precursor protein mice and in humans with cerebral amyloid angiopathy. Stroke J Cereb Circ 43(2):514–523
14. Du H, Li P, Wang J, Qing X, Li W (2012) The interaction of amyloid beta and the receptor for advanced glycation endproducts induces matrix metalloproteinase-2 expression in brain endothelial cells. Cell Mol Neurobiol 32(1):141–147
15. Chisari M, Merlo S, Sortino M, Salomone S (2010) Long-term incubation with beta-amyloid peptides impairs endothelium-dependent vasodilatation in isolated rat basilar artery. Pharmacol Res 61(2):157–161
16. Kuznetsova E, Schliebs R (2013) Beta-amyloid, cholinergic transmission, and cerebrovascular system—a developmental study in a mouse model of Alzheimer's disease. Curr Pharm Des 19(38):6749–6765
17. Kook SY, Hong HS, Moon M, Ha CM, Chang S, Mook-Jung I (2012) Abeta1-42-RAGE interaction disrupts tight junctions of the blood-brain barrier via Ca(2)(+)-calcineurin signaling. J Neurosci 32(26):8845–8854
18. Townsend KP, Obregon D, Quadros A, Patel N, Volmar C, Paris D, Mullan M (2002) Proinflammatory and vasoactive effects of Abeta in the cerebrovasculature. Ann N Y Acad Sci 977:65–76
19. Rombouts SA, Goekoop R, Stam CJ, Barkhof F, Scheltens P (2005) Delayed rather than decreased BOLD response as a marker for early Alzheimer's disease. NeuroImage 26(4):1078–1085
20. Bulbarelli A, Lonati E, Brambilla A, Orlando A, Cazzaniga E, Piazza F, Ferrarese C, Masserini M, Sancini G (2012) Abeta42 production in brain capillary endothelial cells after oxygen and glucose deprivation. Mol Cell Neurosci 49(4):415–422
21. Celsi F, Pizzo P, Brini M, Leo S, Fotino C, Pinton P, Rizzuto R (2009) Mitochondria, calcium and cell death: a deadly triad in neurodegeneration. Biochim Biophys Acta 1787(5):335–344
22. Berridge MJ (2013) Dysregulation of neural calcium signaling in Alzheimer disease, bipolar disorder and schizophrenia. Prion 7(1):2–13
23. Garwood C, Faizullabhoy A, Wharton SB, Ince PG, Heath P, Shaw PJ, Baxter L, Gelsthorpe C, Forster G, Matthews FE, Brayne C, Simpson JE (2013) Calcium dysregulation in relation to Alzheimer-type pathology in the ageing brain. Neuropathol Appl Neurobiol 39(7):788–799
24. Riera J, Hatanaka R, Uchida T, Ozaki T, Kawashima R (2011) Quantifying the uncertainty of spontaneous Ca2+ oscillations in astrocytes: particulars of Alzheimer's disease. Biophys J 101(3):554–564
25. Katayama T, Imaizumi K, Manabe T, Hitomi J, Kudo T, Tohyama M (2004) Induction of neuronal death by ER stress in Alzheimer's disease. J Chem Neuroanat 28(1–2):67–78
26. Yukioka F, Matsuzaki S, Kawamoto K, Koyama Y, Hitomi J, Katayama T, Tohyama M (2008) Presenilin-1 mutation activates the signaling pathway of caspase-4 in endoplasmic reticulum stress-induced apoptosis. Neurochem Int 52(4–5):683–687
27. Supnet C, Bezprozvanny I (2011) Presenilins function in ER calcium leak and Alzheimer's disease pathogenesis. Cell Calcium 50(3):303–309
28. Hedskog L, Pinho CM, Filadi R, Ronnback A, Hertwig L, Wiehager B, Larssen P, Gellhaar S, Sandebring A, Westerlund M, Graff C, Winblad B, Galter D, Behbahani H, Pizzo P, Glaser E, Ankarcrona M (2013) Modulation of the endoplasmic reticulum-mitochondria interface in Alzheimer's disease and related models. Proc Natl Acad Sci U S A 110(19):7916–7921
29. Schon EA, Area-Gomez E (2013) Mitochondria-associated ER membranes in Alzheimer disease. Mol Cell Neurosci 55:26–36
30. Jaworska A, Dzbek J, Styczynska M, Kuznicki J (2013) Analysis of calcium homeostasis in fresh lymphocytes from patients with sporadic Alzheimer's disease or mild cognitive impairment. Biochim Biophys Acta 1833(7):1692–1699

31. Lam AK, Galione A (2013) The endoplasmic reticulum and junctional membrane communication during calcium signaling. Biochim Biophys Acta 1833(11):2542–2559
32. Ferreiro E, Oliveira CR, Pereira CMF (2008) The release of calcium from the endoplasmic reticulum induced by amyloid-beta and prion peptides activates the mitochondrial apoptotic pathway. Neurobiol Dis 30:331–342
33. Fonseca ACRG, Ferreiro E, Oliveira CR, Cardoso SM, Pereira CF (2013) Activation of the endoplasmic reticulum stress response by the amyloid-beta 1-40 peptide in brain endothelial cells. BBA Mol Basis Dis 1832:2191–2203
34. Carvalho C, Correia SC, Santos RX, Cardoso S, Moreira PI, Clark TA, Zhu X, Smith MA, Perry G (2009) Role of mitochondrial-mediated signaling pathways in Alzheimer disease and hypoxia. J Bioenerg Biomembr 41(5):433–440
35. De Bock M, Wang N, Decrock E, Bol M, Gadicherla AK, Culot M, Cecchelli R, Bultynck G, Leybaert L (2013) Endothelial calcium dynamics, connexin channels and blood-brain barrier function. Prog Neurobiol 108:1–20
36. Leadsham JE, Sanders G, Giannaki S, Bastow EL, Hutton R, Naeimi WR, Breitenbach M, Gourlay CW (2013) Loss of cytochrome c oxidase promotes RAS-dependent ROS production from the ER resident NADPH oxidase, Yno1p, in yeast. Cell Metab 18(2):279–286
37. Grammas P, Martinez J, Miller B (2011) Cerebral microvascular endothelium and the pathogenesis of neurodegenerative diseases. Expert Rev Mol Med 13:e19
38. Isenovic E, Soskic S, Dungen HD, Dobutovic B, Elvis T, Simone I, Marche P (2011) Regulation of endothelial nitric oxide synthase in pathophysiological conditions. Cardiovasc Hematol Disord Drug Targets 11(2):109–118
39. Galan C, Jardin I, Dionisio N, Salido G, Rosado JA (2010) Role of oxidant scavengers in the prevention of Ca(2)+ homeostasis disorders. Molecules (Basel, Switzerland) 15(10):7167–7187
40. Ferreiro E, Baldeiras I, Ferreira IL, Costa RO, Rego AC, Pereira CF, Oliveira CR (2012) Mitochondrial- and endoplasmic reticulum-associated oxidative stress in Alzheimer's disease: from pathogenesis to biomarkers. Int J Cell Biol 2012:735206
41. Moreira PI, Duarte AI, Santos MS, Rego AC, Oliveira CR (2009) An integrative view of the role of oxidative stress, mitochondria and insulin in Alzheimer's disease. J Alzheimers Dis 16(4):741–761
42. Pagani L, Eckert A (2011) Amyloid-Beta interaction with mitochondria. Int J Alzheimers Dis 2011:925050
43. Pluta R, Furmaga-Jablonska W, Maciejewski R, Ulamek-Koziol M, Jablonski M (2013) Brain ischemia activates beta- and gamma-secretase cleavage of amyloid precursor protein: significance in sporadic Alzheimer's disease. Mol Neurobiol 47(1):425–434
44. Fonseca ACRG, Proença T, Resende R, Oliveira CR, Pereira CMF (2009) Neuroprotective effects of statins in an in vitro model of Alzheimer's disease. J Alzheimers Dis 17:503–517
45. Guglielmotto M, Aragno M, Autelli R, Giliberto L, Novo E, Colombatto S, Danni O, Parola M, Smith MA, Perry G, Tamagno E, Tabaton M (2009) The up-regulation of BACE1 mediated by hypoxia and ischemic injury: role of oxidative stress and HIF1alpha. J Neurochem 108(4):1045–1056
46. Feine I, Pinkas I, Salomon Y, Scherz A (2012) Local oxidative stress expansion through endothelial cells—a key role for gap junction intercellular communication. PLoS One 7(7):e41633
47. Huppert J, Closhen D, Croxford A, White R, Kulig P, Pietrowski E, Bechmann I, Becher B, Luhmann HJ, Waisman A, Kuhlmann CR (2010) Cellular mechanisms of IL-17-induced blood-brain barrier disruption. Faseb J 24(4):1023–1034
48. El Assar M, Angulo J, Rodriguez-Manas L (2013) Oxidative stress and vascular inflammation in aging. Free Radic Biol Med 65:380–401
49. Fonseca AC, Oliveira CR, Pereira CF, Cardoso SM (2014) Loss of proteostasis induced by amyloid beta peptide in brain endothelial cells. BBA Mol Cell Res 1843(6):1150–1161
50. Bonora M, Giorgi C, Bononi A, Marchi S, Patergnani S, Rimessi A, Rizzuto R, Pinton P (2013) Subcellular calcium measurements in mammalian cells using jellyfish photoprotein aequorin-based probes. Nat Protoc 8(11):2105–2118
51. De Marchi E, Bonora M, Giorgi C, Pinton P (2014) The mitochondrial permeability transition pore is a dispensable element for mitochondrial calcium efflux. Cell Calcium
52. Cathcart R, Schwiers E, Ames B (1983) Detection of picomole levels of hydroperoxides using a fluorescent dichlorofluorescein assay. Anal Biochem 134:111–116
53. Chen X, Zhong Z, Xu Z, Chen L, Wang Y (2010) 2′,7′-Dichlorodihydrofluorescein as a fluorescent probe for reactive oxygen species measurement: forty years of application and controversy. Free Radic Res 44(6):587–604
54. Ribeiro M, Rosenstock TR, Cunha-Oliveira T, Ferreira IL, Oliveira CR, Rego AC (2012) Glutathione redox cycle dysregulation in Huntington's disease knock-in striatal cells. Free Radic Biol Med 53(10):1857–1867
55. Pluta R, Kida E, Lossinsky AS, Golabek AA, Mossakowski MJ, Wisniewski HM (1994) Complete cerebral ischemia with short-term survival in rats induced by cardiac arrest. I. Extracellular accumulation of Alzheimer's beta-amyloid protein precursor in the brain. Brain Res 649(1–2):323–328
56. Pluta R (2006) Is the ischemic blood-brain barrier insufficiency responsible for full-blown Alzheimer's disease? Neurol Res 28(6): 665–671
57. Xu W, Xu F, Anderson ME, Kotarba AE, Davis J, Robinson JK, Van Nostrand WE (2014) Cerebral microvascular rather than parenchymal amyloid-beta protein pathology promotes early cognitive impairment in transgenic mice. J Alzheimers Dis 38(3):621–632
58. Lupo G, Anfuso CD, Assero G, Strosznajder RP, Walski M, Pluta R, Alberghina M (2001) Amyloid beta(1-42) and its beta(25-35) fragment induce in vitro phosphatidylcholine hydrolysis in bovine retina capillary pericytes. Neurosci Lett 303(3):185–188
59. Anfuso CD, Assero G, Lupo G, Nicotra A, Cannavo G, Strosznajder RP, Rapisarda P, Pluta R, Alberghina M (2004) Amyloid beta(1-42) and its beta(25-35) fragment induce activation and membrane translocation of cytosolic phospholipase A2 in bovine retina capillary pericytes. Biochim Biophys Acta 1686(1–2):125–138
60. Lesné S, Koh MT, Kotilinek L, Kayed R, Glabe CG, Yang A, Gallagher M, Ashe KH (2006) A specific amyloid-beta protein assembly in the brain impairs memory. Nature 440(7082):352–357
61. Resende R, Ferreiro E, Pereira C, Oliveira CR (2008) Neurotoxic effect of oligomeric and fibrillar species of Aβ1-42 peptide: involvement of endoplasmic reticulum calcium release in oligomers-induced cell death. Neuroscience 155(3):725–737
62. Chafekar SM, Hoozemans JJ, Zwart R, Baas F, Scheper W (2007) Abeta 1-42 induces mild endoplasmic reticulum stress in an aggregation state-dependent manner. Antioxid Redox Signal 9(12):2245–2254
63. Kirkitadze MD, Bitan G, Teplow DB (2002) Paradigm shifts in Alzheimer's disease and other neurodegenerative disorders: the emerging role of oligomeric assemblies. J Neurosci Res 69(5): 567–577
64. Zhao LN, Long H, Mu Y, Chew LY (2012) The toxicity of amyloid beta oligomers. Int J Mol Sci 13(6):7303–7327
65. Zeiger W, Vetrivel KS, Buggia-Prevot V, Nguyen PD, Wagner SL, Villereal ML, Thinakaran G (2013) Ca2+ influx through store-operated Ca2+ channels reduces Alzheimer disease beta-amyloid peptide secretion. J Biol Chem 288(37):26955
66. Arduino DM, Esteves AR, Domingues AF, Pereira CM, Cardoso SM, Oliveira CR (2009) ER-mediated stress induces mitochondrial-dependent caspases activation in NT2 neuron-like cells. BMB Rep 42(11):719–724
67. Deniaud A, Sharaf eO, Maillier E, Poncet D, Kroemer G, Lemaire C, Brenner C (2008) Endoplasmic reticulum stress induces calcium-

dependent permeability transition, mitochondrial outer membrane permeabilization and apoptosis. Oncogene 27(3):285–299
68. Giorgi C, De Stefani D, Bononi A, Rizzuto R, Pinton P (2009) Structural and functional link between the mitochondrial network and the endoplasmic reticulum. Int J Biochem Cell Biol 41(10): 1817–1827
69. Chakroborty S, Briggs C, Miller MB, Goussakov I, Schneider C, Kim J, Wicks J, Richardson JC, Conklin V, Cameransi BG, Stutzmann GE (2012) Stabilizing ER Ca2+ channel function as an early preventative strategy for Alzheimer's disease. PLoS One 7(12):e52056
70. Patergnani S, Suski JM, Agnoletto C, Bononi A, Bonora M, De Marchi E, Giorgi C, Marchi S, Missiroli S, Poletti F, Rimessi A, Duszynski J, Wieckowski MR, Pinton P (2011) Calcium signaling around Mitochondria Associated Membranes (MAMs). Cell Commun Signal 9:19
71. Giorgi C, Baldassari F, Bononi A, Bonora M, De Marchi E, Marchi S, Missiroli S, Patergnani S, Rimessi A, Suski JM, Wieckowski MR, Pinton P (2012) Mitochondrial Ca(2+) and apoptosis. Cell Calcium 52(1):36–43
72. Solito R, Corti F, Chen CH, Mochly-Rosen D, Giachetti A, Ziche M, Donnini S (2013) Mitochondrial aldehyde dehydrogenase-2 activation prevents beta-amyloid-induced endothelial cell dysfunction and restores angiogenesis. J Cell Sci 126(Pt 9):1952–1961
73. Fossati S, Ghiso J, Rostagno A (2012) Insights into caspase-mediated apoptotic pathways induced by amyloid-beta in cerebral microvascular endothelial cells. Neurodegener Dis 10(1–4):324–328
74. Hsu MJ, Sheu JR, Lin CH, Shen MY, Hsu CY (2010) Mitochondrial mechanisms in amyloid beta peptide-induced cerebrovascular degeneration. Biochim Biophys Acta 1800(3):290–296
75. Cioffi DL, Stevens T (2006) Regulation of endothelial cell barrier function by store-operated calcium entry. Microcirculation 13(8): 709–723
76. Gosselet F, Saint-Pol J, Candela P, Fenart L (2013) Amyloid-beta peptides, Alzheimer's disease and the blood-brain barrier. Curr Alzheimer Res 10(10):1015–1033
77. Groschner LN, Waldeck-Weiermair M, Malli R, Graier WF (2012) Endothelial mitochondria—less respiration, more integration. Pflugers Arch 464(1):63–76
78. Jornot L, Maechler P, Wollheim CB, Junod AF (1999) Reactive oxygen metabolites increase mitochondrial calcium in endothelial cells: implication of the Ca2+/Na+ exchanger. J Cell Sci 112(Pt 7): 1013–1022
79. Cornejo VH, Hetz C (2013) The unfolded protein response in Alzheimer's disease. Semin Immunopathol 35(3):277–292
80. Viana RJ, Nunes AF, Rodrigues CM (2012) Endoplasmic reticulum enrollment in Alzheimer's disease. Mol Neurobiol 46(2):522–534
81. Bintig W, Begandt D, Schlingmann B, Gerhard L, Pangalos M, Dreyer L, Hohnjec N, Couraud PO, Romero IA, Weksler BB, Ngezahayo A (2012) Purine receptors and Ca(2+) signalling in the human blood-brain barrier endothelial cell line hCMEC/D3. Purinergic Signal 8(1):71–80
82. Park WH (2012) The effects of exogenous H2O2 on cell death, reactive oxygen species and glutathione levels in calf pulmonary artery and human umbilical vein endothelial cells. Int J Mol Med 31(2):471–476
83. Ferreiro E, Resende R, Costa R, Oliveira CR, Pereira CMF (2006) An endoplasmic-reticulum-specific apoptotic pathway is involved in prion and amyloid-beta peptides neurotoxicity. Neurobiol Dis 23: 669–678
84. Carvalho C, Katz PS, Dutta S, Katakam PV, Moreira PI, Busija DW (2013) Increased susceptibility to amyloid-beta toxicity in rat brain microvascular endothelial cells under hyperglycemic conditions. J Alzheimers Dis 38(1):75–83
85. Hetz C (2012) The unfolded protein response: controlling cell fate decisions under ER stress and beyond. Nat Rev Mol Cell Biol 13(2): 89–102
86. Lagace TA, Ridgway ND (2013) The role of phospholipids in the biological activity and structure of the endoplasmic reticulum. BBA Mol Cell Res 1833(11):2499–2510
87. Ron D, Harding HP (2013) Protein-folding homeostasis in the endoplasmic reticulum and nutritional regulation. Cold Spring Harb Perspect Biol 4(12)
88. Cullinan SB, Diehl JA (2006) Coordination of ER and oxidative stress signaling: the PERK/Nrf2 signaling pathway. Int J Biochem Cell Biol 38(3):317–332
89. Harding HP, Zhang Y, Zeng H, Novoa I, Lu PD, Calfon M, Sadri N, Yun C, Popko B, Paules R, Stojdl DF, Bell JC, Hettmann T, Leiden JM, Ron D (2003) An integrated stress response regulates amino acid metabolism and resistance to oxidative stress. Mol Cell 11: 619–633
90. Ogawa Y, Saito Y, Nishio K, Yoshida Y, Ashida H, Niki E (2008) Gamma-tocopheryl quinone, not alpha-tocopheryl quinone, induces adaptive response through up-regulation of cellular glutathione and cysteine availability via activation of ATF4. Free Radic Res 42(7): 674–687
91. Warabi E, Takabe W, Minami T, Inoue K, Itoh K, Yamamoto M, Ishii T, Kodama T, Noguchi N (2007) Shear stress stabilizes NF-E2-related factor 2 and induces antioxidant genes in endothelial cells: role of reactive oxygen/nitrogen species. Free Radic Biol Med 42(2):260–269
92. Bonello S, Zahringer C, BelAiba RS, Djordjevic T, Hess J, Michiels C, Kietzmann T, Gorlach A (2007) Reactive oxygen species activate the HIF-1alpha promoter via a functional NFkappaB site. Arterioscler Thromb Vasc Biol 27(4):755–761
93. Fong GH (2009) Regulation of angiogenesis by oxygen sensing mechanisms. J Mol Med (Berlin, Germany) 87(6):549–560
94. Bell EL, Klimova TA, Eisenbart J, Schumacker PT, Chandel NS (2007) Mitochondrial reactive oxygen species trigger hypoxia-inducible factor-dependent extension of the replicative life span during hypoxia. Mol Cell Biol 27(16):5737–5745
95. Jung SN, Yang WK, Kim J, Kim HS, Kim EJ, Yun H, Park H, Kim SS, Choe W, Kang I, Ha J (2008) Reactive oxygen species stabilize hypoxia-inducible factor-1 alpha protein and stimulate transcriptional activity via AMP-activated protein kinase in DU145 human prostate cancer cells. Carcinogenesis 29(4):713–721
96. Sarada SK, Himadri P, Ruma D, Sharma SK, Pauline T, Mrinalini (2008) Selenium protects the hypoxia induced apoptosis in neuroblastoma cells through upregulation of Bcl-2. Brain Res 1209:29–39
97. Taylor CT (2008) Mitochondria and cellular oxygen sensing in the HIF pathway. Biochem J 409(1):19–26
98. Bota DA, Alexandru D, Keir ST, Bigner D, Vredenburgh J, Friedman HS (2013) Proteasome inhibition with bortezomib induces cell death in GBM stem-like cells and temozolomide-resistant glioma cell lines, but stimulates GBM stem-like cells' VEGF production and angiogenesis. J Neurosurg 119(6):1415–1423
99. Tajima M, Kurashima Y, Sugiyama K, Ogura T, Sakagami H (2009) The redox state of glutathione regulates the hypoxic induction of HIF-1. Eur J Pharmacol 606(1–3):45–49
100. Mobasheri A, Richardson S, Mobasheri R, Shakibaei M, Hoyland JA (2005) Hypoxia inducible factor-1 and facilitative glucose transporters GLUT1 and GLUT3: putative molecular components of the oxygen and glucose sensing apparatus in articular chondrocytes. Histol Histopathol 20(4):1327–1338